HHS Public Access

Author manuscript

Biol Psychiatry. Author manuscript; available in PMC 2017 December 01.

Published in final edited form as:

Biol Psychiatry. 2016 December 01; 80(11): 878–887. doi:10.1016/j.biopsych.2016.02.031.

Gamma-Aminobutyric Acidergic Projections From the Dorsal Raphe to the Nucleus Accumbens Are Regulated by Neuromedin U

James M. Kasper[1], **David L. McCue**[1], **Adrianna J. Milton**[1], **Angelia Szwed**[1], **Catherine M. Sampson**[1], **Mei Huang**[3], **Susan Carlton**[2], **Herbert Y. Meltzer**[3], **Kathryn A. Cunningham**[1], and **Jonathan D. Hommel**[1,*]

[1]Center for Addiction Research, Department of Pharmacology & Toxicology, University of Texas Medical Branch, Galveston, Texas, 77555, USA

[2]Department of Neuroscience and Cell Biology, University of Texas Medical Branch, Galveston, Texas, 77555, USA

[3]Department of Psychiatry and Behavioral Sciences, Northwestern Feinberg School of Medicine, Chicago, Illinois, 60611, USA

Abstract

Introduction—Neuromedin U (NMU) is a neuropeptide enriched in the nucleus accumbens shell (NAcSh), a brain region associated with reward. While NMU and its receptor, NMU Receptor 2 (NMUR2), have been studied for its ability to regulate food reward, NMU has not been studied in the context of drugs of abuse (e.g. cocaine). Furthermore, the neuroanatomical pathways which express NMUR2 and its ultrastructural localization are unknown.

Methods—Immunohistochemistry was used to determine the synaptic localization of NMUR2 in the NAcSh and characterize which neurons express this receptor (n=17). The functional outcome of NMU on NMUR2 was examined using microdialysis (n=16). The behavioral effects of NMU microinjection directly to the NAcSh was investigated using cocaine-evoked locomotion (n=93). The specific effects of NMUR2 knockdown on cocaine-evoked locomotion was evaluated using viral-mediated RNAi (n=40).

*Correspondence: jdhommel@utmb.edu, Jonathan D. Hommel, University of Texas Medical Branch, 301 University Blvd., Galveston, TX 77555-0615.

Author Contributions

J.M.K., D.L.M., A.J.M., A.S. and C.M.S. performed the immunohistochemistry. S.C. contributed the electron microscopy. J.M.K. and D.L.M. performed the surgeries. J.M.K. preformed the behavior experiments. M.H. quantified the microdialysis samples. J.M.K., A.J.M., M.H. and J.D.H. performed the data analysis. J.M.K., S.C. and J.D.H. drafted the manuscript. J.M.K., S.C., H.Y.M, K.A.C. and J.D.H conceived the experiments. All have edited the manuscript.

Conflicts of Interest

The authors report no biomedical financial interests or potential conflicts of interest.

Results—NMUR2 is localized to presynaptic GABAergic nerve terminals in the NAcSh originating from the dorsal raphe nucleus. Furthermore, NMU microinjection to the NAcSh decreased local GABA concentrations. Next, we evaluated the effects of NMU microinjection on behavioral sensitization to cocaine. When repeatedly administered throughout the sensitization regimen, NMU attenuated cocaine-evoked hyperactivity. Additionally, shRNA-mediated knockdown of presynaptic NMUR2 in the NAcSh using a retrograde viral vector potentiated cocaine sensitization.

Conclusions—Together, these data reveal that NMUR2 modulates a novel GABAergic pathway from the dorsal raphe nucleus to the NAcSh to influence behavioral responses to cocaine.

Keywords

Neuropeptide; nonserotonergic; GABA; cocaine; AAV6; RNAi

Neuromedin U Receptor 2 (NMUR2) is a highly conserved G protein-coupled receptor (1) expressed in the central nervous system (2–4). NMUR2 and its endogenous ligand, the neuropeptide Neuromedin U (NMU) (5, 6), have primarily been studied for their role in regulating food intake (5, 7). Compelling evidence suggests that obesity and addiction processes involve overlapping neurocircuits, particularly within brain reward centers (8–10). This overlap may involve NMU signaling. NMU and NMUR2 are enriched in the nucleus accumbens (NAc) (11), particularly, the NAc shell (NAcSh) which is a key component in brain circuitry underlying reinforcement and other drug-evoked behaviors (12–16). Microarray studies have identified NMU as a transcript regulated by acute methamphetamine exposure (17) in rats and a single nucleotide polymorphism in *Nmur2* is associated with alcoholism (18) in humans. Despite these intriguing data, the enrichment of NMUR2 in the NAcSh, and the importance of the NAcSh in animal models of substance use disorders, no functional or mechanistic studies have investigated NMU/NMUR2 in the context of drug related neurocircuitry or behaviors. This gap in knowledge represents an opportunity to explore NMUR2 as a novel regulator of key addiction related pathways of the brain.

In the present study, we explored the neurocircuitry that expresses NMUR2 in the NAcSh using immunohistochemistry and viral tracers to establish and characterize NMUR2-positive pathways between the NAcSh and other brain regions associated with addiction (19) such as the dorsal raphe nucleus (DRN), caudate putamen (CPu), amygdala (AMG), or tail of the ventral tegmental area (tVTA). Next, the effect of NMU on neurotransmitter release in the NAcSh was evaluated to verify the functional output of NMU signaling. The behavioral relevance of the changes in neurotransmission following accumbal administration of NMU was modeled using behavioral sensitization to cocaine. Behavioral sensitization is a progressive enhancement of the behavioral effects (e.g., locomotor hyperactivity) driven by repeated exposure to a psychostimulant. The repeated drug exposure serves to study the neural basis of altered responsiveness to drugs (13). This non-response contingent model involves pathways that have been demonstrated to play a key role in models of relapse and has been used to identify and screen potential pharmacotherapeutic targets (13) and involved neurocircuitry (20). The functional significance of NMUR2 was evaluated using an *in vivo* knockdown of presynaptic NMUR2 in the NAcSh and examining behavioral sensitization to

cocaine. This work represents the first step in characterizing NMUR2-positive pathways and determining the behavioral relevance of this neurocircuitry.

Materials and Methods

Animals

Male Sprague-Dawley rats (n=166 total, Harlan, Indianapolis, IN) weighing 225 to 250 g, were singly housed. Rat use was carried out in accordance with the Guide for the Care and Use of Laboratory Animals and with the approval of the University of Texas Medical Branch Institutional Animal Care and Use Committee.

Electron microscopy

We evaluated the localization of NMUR2 in the NAcSh region using postembedding immunogold staining (21–23). A protocol for immunogold staining has been previously published by our lab (24, 25). Briefly, rats (n=3) were perfused, the brain was removed and the tissue blocks were post fixed, embedded with epon, cured, cut and rinsed. The grids were place on drops of the following solutions: normal goat serum diluted in Tris buffer (5%, 1 hour); NMUR2 antiserum (1:25, Novus Biologicals, Littleton, CO; NBP1-02351, 24 hours), goat anti-rabbit IgG-gold (20 nm, Ted Pella, Redding, CA; 1 hour), rinsed and post-stained prior to analysis. Specificity of the NMUR2 antibody was previously validated (26). Additionally, grids incubated in diluent lacking the primary antisera resulted in a complete lack of immunogold staining on the grids. Using a JEOL 1400 EM scope, all gold-labeled profiles within randomly chosen screens in the region encompassing the NAcSh were photographed and 166 photos were analyzed.

Immunohistochemistry

Colocalization of the tracer virus expressing green fluorescent protein (GFP) with NMUR2 in the NAcSh was visualized using fluorescent immunohistochemistry (26). Briefly, the sections were unmasked, blocked and incubated in primary antibodies. The primary antibodies included rabbit αNMUR2 (1:150; Novus Biologicals, Littleton, CO; NBP1-02351), chicken αGFP (1:500; Aves Labs, Tigard, OR; GFP1020). Sections were incubated with secondary antibody goat αrabbit AF-555 (1:100; Life Technologies, Carlsbad, CA; A21429) and donkey αchicken AF-488 (1:100; Jackson ImmunoResearch, West Grove, PA; 703-545-155) for 2 hours.

Colocalization of NMUR2 with glutamic acid decarboxylase 67 (GAD67), tryptophan hydroxylase (TPH) and tyrosine hydroxylase (TH) in the NAcSh was also visualized. The procedure was performed as above using the following primary antibodies: rabbit αNMUR2 (as previous), mouse αGAD67 (1:150; Abcam, United Kingdom; ab26116), mouse αTPH (1:1000; Sigma, St. Louis, MO; T0678), and mouse αTH (1:500; Sigma, St. Louis, MO; T2928). Secondary antibodies included donkey αrabbit AF-488 (1:200; Jackson ImmunoResearch, West Grove, PA; 711-546-152) and donkey αmouse AF-555 (1:200; Invitrogen, Carlsbad, CA; A31570).

Triple colocalization of NMUR2, tracer from the DRN, and GAD67 was performed as described above. The secondary antibodies included goat αrabbit cascade blue (1:200, Life Technologies, Carlsbad, CA; C-2764), donkey αchicken AF-488 (as previous), and donkey αmouse AF-555 (as pervious).

All images for colocalization were acquired using Leica True Confocal Scanner SPE and Leica Application Suite Advanced software (Leica Microsystems, Germany). Images were pseudocolored and image colocalization was quantified using ImageJ with JACoP (27) software. The moments (28) auto thresholding option was applied to all images and the Manders' M2 coefficient was calculated for either the fraction of 1) NMUR2 immunofluorescent pixels that colocalize with the tracer or 2) neuronal tracer that colocalizes with NMUR2. The statistical differences were tested using ANOVA with Tukey post hoc test on Prism 6 software (GraphPad Software, Inc, La Jolla, CA).

Microdialysis

Each rat was anesthetized and placed in a stereotaxic instrument (Kopf) for implantation of guide cannula. The microdialysis probe guide cannula (CMA Microdialysis, Sweden) and microinjection guide cannula (PlasticsOne, Roanoke, VA) were anchored with two stainless steel screws and dental cement. Coordinates for microdialysis and NMU microinjections are detailed in Figure S1. The dual cannula setup was used instead of reverse dialysis in consideration of probe molecular weight cutoff and dialysate analysis. After recovery, CMA 11 microdialysis probes, with 2mm active length, were perfused with artificial cerebrospinal fluid (aCSF) at 1 μL/min. Probe was inserted and rats were allowed to freely move around the CMA 120 system. Two hours after implantation (29), samples were collected every 30 minutes.

Neurotransmitters were assayed by UPLC and MS/MS (30). The LC system (Waters Acquity UPLC, Waters Co., Milford, MA) with a binary solvent manager, sample organizer, sample manager and column manager and a Waters Acquity UPLC HSS T3 1.8 μm column were used for the separation. The UPLC system was coupled to a triple-quadrupole mass spectrometer (Thermo TSQ Quantum Ultra, Carlsbad, CA), using electrospray ionization in positive mode. All data were processed by Waters MassLynx 4.0 and Thermo Xcaliber software. Data were acquired and analyzed using Thermo LCquan 2.5 software (Thermo Fisher Scientific, Inc., Carlsbad, CA). Repeated measures ANOVA with planned comparisons were performed.

NAcSh cannulation and microinjection

Rat (n=93) surgery and cannula implantation was performed similar to the microdialysis experiment. Rats were habituated to being held by hand and microinjections of aCSF or 0.3 nmol NMU (porcine 8-mer sequence, GenScript, Township, NJ) in aCSF were administered at 1 μl per minute for 2 minutes.

Sensitized locomotor activity

Sensitization was achieved using a previous method (31). Briefly, all rats were given a saline injection and locomotor activity was measured to determine basal locomotion using an open-

field enclosure and photobeam matrix (San Diego Instruments, San Diego, CA). During pretreatment phase, rats received twice per day i.p. injections of saline or 15 mg/kg cocaine and the following hour of locomotor activity was measured. Animals were then left untreated for one week. Challenge day locomotor activity was analyzed using ANOVA and planned comparisons.

Virus injections

Rats (n=40) were anesthetized and placed in a stereotaxic instrument similar to the previous cannulation procedure for the viral injections. The knockdown vector used was an AAV6 with shRNA against *Nmur2* or scrambled shRNA control (26) that was microinjected bilaterally into the NAcSh. Total microinjection volume for NAcSh was 2 μL. The tracer vector used was an AAV2 that expresses a fusion protein of synaptobrevin and GFP (32). Microinjections of tracer into the DRN: −7.1mm anteroposterior, +3.2mm lateral, and −7.3mm dorsoventral with a 30° angle, tVTA: −5.6mm anteroposterior, +1.6mm lateral, and −8.2mm dorsoventral with a 0° angle, AMG: −3.3mm anteroposterior, +5.0mm lateral, and −8.5mm dorsoventral with a 0° angle, or CPu: +2.3mm anteroposterior, +2.4mm lateral, and −4.6mm dorsoventral with a 0° angle. All coordinates were chosen according to Paxinos and Watson (33).

Results

NMUR2 is expressed presynaptically in the NAcSh

To gain a greater understanding of how NMU in the NAcSh modulates the behavioral effects of cocaine, we evaluated the underlying neuronal architecture of NMUR2-containing neurons using fluorescence immunohistochemistry to visualize NMUR2 expression in the NAcSh. The image (Figure 1A), at 63× magnification, shows immunohistochemical staining with a “beads on a string” motif suggesting presynaptic receptor expression (34). To confirm presynaptic expression, we used electron microscopy immunogold labeling to identify the synaptic localization of NMUR2 in the NAcSh (Figure 1B). Staining for NMUR2 is highlighted with blue arrows. The mean percentage of gold-labeled profiles were determined by analyzing 166 digital images of the NAcSh containing 1 to 4 NMUR2 positive processes each. The lumen of blood vessels in the NAcSh region were checked for non-specific binding and had no gold particles in them, indicating extremely low non-specific binding. In general, gold labeling was observed on axonal profiles (Figure 1B). A gold particle was considered to be associated with a synaptic specialization if the particle was <50 nm from the synapse and was considered perisynaptic if 50–150 nm from the synapse (35). Using these criteria, 28% of the gold particles represented synaptic labeling, 28% perisynaptic, and 44% nonsynaptic (Figure 1C). When present, the labeling for NMUR2 was in the presynaptic element (71%), which could be identified as an axonal bouton; 29% of the label was on the postsynaptic side, which was identified as a dendritic spine or small diameter dendrite (36) (Figure 1C). These data suggest that NMUR2 exerts its effects upon presynaptic terminals in the NAcSh.

NMUR2 colocalizes with projections from the DRN and GAD67

To define the neuronal pathways innervating the NAcSh that express NMUR2, we utilized an AAV2 vector that expresses a synaptobrevin-GFP fusion protein (32). Synaptobrevin is a vesicle fusion protein that is transported from the cell body to presynaptic terminals (37); GFP facilitates visualization, to label synaptic terminals of neurons that originate from the site of viral injection. This vector-based tracer was injected into areas of the brain that express *Nmur2* mRNA and send efferent projections to the NAcSh, namely the DRN, tVTA, AMG, and CPu (Figure 2A). Brains of these animals were collected and processed for confocal microscopy. Images of the NAcSh were quantified using ImageJ with JACoP (27) software and the fraction of NMUR2 immunofluorescent pixels that colocalize with GFP-labeled axon terminals compared to total NMUR2 (Figure 2B). These data revealed colocalization of NMUR2 predominantly in axons originating in the DRN (ANOVA main effect $F(3,28)=6.37$, $p=0.002$; Figure 2C).

Upon learning that NMUR2 is localized to axons projecting from the DRN, we sought to define the neuronal sub-type expressing NMUR2. Key neurotransmitters in the NAcSh involved in cocaine related behaviors are GABA, serotonin, and dopamine (38–43). To this end, we evaluated NMUR2 colocalization with markers for GABA, serotonin, and dopamine neurons using GAD67, TPH and TH, antibodies respectively (Figure 3A). Quantification of the colocalization of NMUR2 with the sub-type markers indicates that NMUR2 is found predominantly on GAD67-positive axons (ANOVA main effect $F(2,13)=16.17$, $p=0.0003$; Figure 3B).

To confirm that there is overlap between the NMUR2 projections from the DRN and GABAergic markers, we evaluated triple colocalization in the NAcSh for NMUR2, GFP tracer from the DRN, and GAD67. Confocal images demonstrate the presence of axon terminals in which all three markers colocalize (Figure 4A). This suggests that GABAergic neurons from the DRN project to the NAcSh and presynaptically express NMUR2 (Figure 4B).

NMU decreases GABA in the NAcSh

Knowing that NMUR2 is presynaptically expressed on GABAergic neurons, we explored the effect of NMUR2 activation on neurotransmitter release. To determine the effect of local NMU on neurotransmitter concentrations in the NAcSh, we performed microdialysis in the NAcSh of freely moving, unanesthetized rats. As this is the first experiment to study the effect of NMU microinjection on GABA, the dose of NMU was chosen based on previous studies that established the amount needed to elicit behavioral effects on feeding (44, 45). Here, basal samples were gathered and then NMU or vehicle was microinjected into the NAcSh. Microdialysis probe placement and microinjection sites were recorded (Figure S1A). Samples were quantified using ultra performance liquid chromatography and mass spectrometry (MS/MS) (30). Average basal concentrations of dialysate showed 198 nM GABA, 2 nM serotonin, and 3 nM dopamine before accounting for microdialysis probe recovery. Microdialysis demonstrated that NMU significantly decreases extracellular concentrations of GABA, but not serotonin or dopamine (repeated measures two-way ANOVA with GABA main effects of time ($F(5,55)=1.87$, $p=0.045$) but not NMU treatment

($F(1,11)=2.13$, $p=0.17$) with planned comparisons) (Figure 5). The effects of NMU on GABA persisted 60 minutes after microinjection before returning to baseline. The NMU-evoked decrease in GABA was supported by immunohistochemistry studies examining the expression of Fos, an immediate early gene. When NMU was microinjected into the NAcSh, increased Fos staining was observed compared to vehicle-injected rats (t-test, $p=0.0104$) (Figure S2). Increased Fos expression is associated with neuronal stimulation which is consistent with decreased GABA concentrations. Thus, NMU-induced increases in Fos is thought to result from disinhibition of NAcSh neurons.

Administration of NMU into the NAcSh attenuates cocaine sensitization

Accumbal GABA can influence motor behavior including locomotion (46). As NMU decreases GABA in the NAcSh, we first established the role of NAcSh NMU on locomotor activity (Figure 6). Here, we microinjected NMU (0.3 nmol per side) or vehicle (aCSF) directly into the NAcSh (Figure S1B). NMU microinjection into the NAcSh does not alter basal locomotor activity (veh vs. NMU; t-test, $p=0.57$) (Figure 6B).

As NMU does not alter basal locomotion, we investigated if NMU can alter cocaine-evoked locomotion. Specifically, we determined the role NMU-NMUR2 signaling in the NAcSh on sensitization to cocaine evoked locomotor activity. Rats were administered a cocaine sensitization regimen of 15 mg/kg intraperitoneally (i.p.) twice a day for five days (Figure 7A), which induces a progressive enhancement of cocaine-evoked hyperactivity during the repeated treatment period (31) (Figure S3A). Following a 7 day abstinence period in which the rats received no treatment, the cocaine-sensitized rats and respective saline controls (1 ml/kg, i.p, 2×/day, 5 days) were microinjected with NMU (0.3 nmol per side) or vehicle directly into the NAcSh (Figure S1B) and all rats were immediately challenged with cocaine (15 mg/kg). Horizontal locomotor activity (total beam breaks over 1 hour) was measured to determine the effect of challenge day NMU upon *expression* of sensitization. Main effects of repeated cocaine treatment ($F(1,25)=30.86$, $p<0.001$) and challenge day NMU ($F(1,25)=9.52$, $p=0.005$) were observed on challenge day locomotion (repeated cocaine×NMU interaction $F(1,25)=1.38$, $p=0.25$). The rats that received the repeated cocaine sensitization regimen displayed enhanced cocaine-evoked hyperactivity compared to saline-treated animals that received an acute cocaine challenge indicating that sensitization did occur (13) (Figure 7B, veh with saline vs. cocaine pretreatment, $p=0.016$). NMU significantly attenuated acute cocaine-evoked hyperactivity in the saline-treated rats (Figure 7B, veh vs. NMU with saline pretreatment; $p=0.025$). Conversely, NMU did not significantly alter the enhanced cocaine-evoked hyperactivity observed in the cocaine-sensitized rats (veh vs. NMU with cocaine pretreatment; $p=0.49$), indicating differential influence of intra-NAcSh NMU on acute cocaine-evoked hyperactivity verses sensitized cocaine-evoked hyperactivity.

To examine the effect of NMU administered during *initiation* of sensitization, NMU (0.3 nmol per side) or vehicle was microinjected into the NAcSh (Figures 7C and S1C) immediately prior to each i.p. administration of cocaine (15 mg/kg or saline, 2×/day, 5 days Figure S3B) during the sensitization treatment regime. Following 7 days of abstinence, all rats were challenged with an acute cocaine injection (15 mg/kg, i.p.) (Figure 7D). A two-

way ANOVA showed main effect of repeated NMU pretreatment ($F(1,32)=15.60$, $p=0.0004$) and repeated cocaine treatment ($F(1,32)=8.96$, $p=0.0055$) on hyperactivity induced by acute cocaine challenge (NMU pretreatment×cocaine treatment interaction $F(1,32)=1.52$, $p=0.23$). Even though rats had not received NMU in over a week, the intra-NAcSh microinjection of NMU administered during the sensitization treatment regimen blocked both acute cocaine-evoked hyperactivity and the sensitized cocaine-evoked hyperactivity on challenge day compared to rats that received vehicle pretreatment (veh vs. NMU pretreatment with saline pretreatment or veh vs. NMU pretreatment with cocaine pretreatment, respectively; $p<0.05$) (Figure 7D). This suggests that enhancement of NMU signaling in the NAcSh in the presence of cocaine induces a protective effect against future cocaine exposure.

Knockdown of presynaptic NMUR2 in NAcSh augments cocaine sensitization

To evaluate the behavioral relevance of the presynaptic subpopulation of NMUR2 in the NAcSh (Figure 1), we selectively targeted neurons expressing presynaptic NMUR2 using an innovative application of viral technology. A non-silencing shRNA control (shCTRL) or a previously validated shRNA designed to knockdown NMUR2 (26) was packaged into an AAV6 viral vector. The AAV6 viral vector is transported in the retrograde direction (47, 48) thus allowing us to knockdown NMUR2 in afferents of the NAcSh (Figure S1D; validation in Figure S4). After the virus was fully expressed (14–17 days), rats underwent a similar cocaine sensitization paradigm as with the NMU microinjection experiments (Figures 8A and S3C). Two-way ANOVA revealed a significant main effect of sh*Nmur2* ($F(1,31)=9.34$, $p=0.005$) and repeated cocaine treatment ($F(1,31)=24.95$, $p<0.0001$) upon cocaine challenge (sh*Nmur2* × repeated cocaine interaction $F(1,31)=1.22$, $p=0.28$). As expected, sensitization of cocaineevoked hyperactivity was observed in the shCTRL rats administered repeated cocaine (shCTRL with saline pretreatment vs. cocaine pretreatment; $p<0.05$) (Figure 8B). Although knockdown of presynaptic NMUR2 had no effect upon acute cocaine-evoked locomotor activity in the saline-treated rats (shCTRL vs. sh*Nmur2* with saline pretreatment; $p=0.51$; n.s. Figure 8B), knockdown of presynaptic NMUR2 in the NAcSh significantly potentiated the sensitization of cocaine-evoked hyperactivity (shCTRL vs. sh*Nmur2* with cocaine pretreatment; $p<0.05$; Figure 8B). These data suggest that presynaptic NMUR2 in the NAcSh functions to suppress cocaine sensitization.

Discussion

Here we describe a GABAergic pathway from the DRN to the NAcSh that is regulated by NMU-NMUR2 signaling. Furthermore, the present study represents the first reported evidence that NMU-NMUR2 signaling modulates cocaine-evoked behavior. Specifically, administration of NMU into the NAcSh during initiation, but not expression, blocks cocaine sensitization through actions on NMUR2. The knockdown of presynaptic NMUR2 potentiating cocaine-evoked hyperactivity emphasizes the importance of NMUR2 in cocaine sensitization. The differential effects of intra-NAcSh NMU when administered during initiation vs. expression of sensitization is likely due to alterations in NMUR2 signaling upon repeated cocaine exposure that are blocked when NMU is simultaneously administered throughout the repeated treatment regimen. This is further supported by our data demonstrating that selective knockdown of presynaptic NAcSh NMUR2 using AAV6 prior

to cocaine exposure significantly potentiates acute cocaine-evoked hyperactivity and cocaine sensitization. Our use of AAV6 represents a technological advancement as the first use of the AAV6 to knockdown presynaptic receptor expression in the brain. This study further supports the convergence of food and cocaine mechanisms on circuitry regulating motivated behavior (8–10, 38), and implicates an important role for NMU signaling in the NAcSh within this overlapping circuitry.

The present data indicate that the behavioral effects of NMU are likely due to reduced local GABA release in the NAcSh. This suggests that NMU in the NAcSh acts through presynaptic NMUR2 to inhibit local GABA release, presumably through Gαi signaling (1). While the role of accumbal GABA in cocaine-evoked behavior has not been fully elucidated, animals in abstinence from repeated cocaine self-administration display increased basal GABA concentrations (39). Furthermore, both rats selfadministering cocaine and their yoked-cocaine treated controls display increased basal GABA in the NAcSh after 10 days of abstinence (49). In addition to these changes in GABA release, cocaine regulates the GABA synthesis enzyme GAD in the NAcSh. Specifically, acute cocaine increases GAD mRNA but repeated cocaine treatment has no effect on GAD mRNA (50). This is consistent with our observations showing that NMU alters acute, but not repeated, cocaine treated behavior (Figure 7B). This suggests that increased GAD expression in the NAcSh during acute cocaine leads to elevated basal levels of GABA (39, 49). Thus, administration of NMU into the NAcSh during repeated cocaine administration (Figure 7D) may indirectly counteract the initial increase in GAD mRNA expression and block neuroadaptations that converge in the NAcSh to drive cocaine sensitization. In addition, others have shown that the GABAA receptor antagonist bicuculline, administered directly to the NAc, attenuates cocaine-evoked locomotion (51). This is consistent with our work and suggests that NMU-induced decreases in GABA concentration in the NAcSh are resulting in a suppression of cocaine-evoked locomotion.

Nonserotonergic projections from the DRN to some brain reward centers, namely the ventral tegmental area, can modulate reinforcement (52). Although a GABAergic pathway from the DRN to the nucleus accumbens has been described in mice (53, 54), the behavioral function and downstream sites of action of this pathway remain poorly understood. Possibly, the GABAergic projections may be targeting dopamine D2 receptor-containing neurons because activation of the indirect pathway results in inhibition of behavioral sensitization (55). In this case, NMUR2 signaling would be decreasing GABA release onto D2 neurons in the NAc resulting in a disinhibition (i.e. activation) of the indirect pathway and a suppression of behavioral sensitization. Overall, this study demonstrates the functional significance of the GABAergic pathway from the DRN to the NAcSh to modulate drug-related behavior. Thus, the DRN can directly modulate addiction-related neuronal substrates through non-serotonergic means via inhibitory GABAergic signaling in the NAcSh.

Together, our data demonstrate a GABAergic pathway from the DRN to the NAcSh that can be modulated through NMUR2 to regulate behavioral sensitization to cocaine. Although the specific source of NMU is unclear, the NAc expresses the highest levels of NMU peptide in the brain (11). Furthermore, microarray studies have identified NMU mRNA as a transcript in the NAc that is stimulated by methamphetamine (56). Thus, NMU-NMUR2 signaling in

the nucleus accumbens may be a feedback signal to dampen the effects of psychostimulants which eventually becomes disrupted following repeated psychostimulant exposure. These findings emphasize the importance of non-serotonergic projections from the DRN to the nucleus accumbens in drug-related behaviors and establish NMUR2 as a novel target in this pathway to modulate cocaine-evoked behavior.

Supplementary Material

Refer to Web version on PubMed Central for supplementary material.

Acknowledgments

We thank Dr. Ralph DiLeone for providing AAV2 synaptobrevin-GFP tracer and Dr. Marcy Jordan for critically editing the manuscript. These results have been previously published as an abstract for oral presentation in *Drug and Alcohol Dependence* 156 (2015) e102–e182. This work was supported by the Weisman Family Foundation, the National Institute on Drug Abuse (R03DA033437, P30DA028821, and T32DA07287); Peter F. McManus Charitable Trust; and Clinical and Translational Science Award (UL1TR001439 and KL2TR001441) from the National Center for Advancing Translational Science.

References

1. Brighton PJ, Szekeres PG, Wise A, Willars GB. Signaling and ligand binding by recombinant neuromedin U receptors: evidence for dual coupling to Galphaq/11 and Galphai and an irreversible ligand-receptor interaction. Mol Pharmacol. 2004; 66:1544–1556. [PubMed: 15331768]
2. Brighton PJ, Szekeres PG, Willars GB. Neuromedin U and its receptors: structure, function, and physiological roles. Pharmacol Rev. 2004; 56:231–248. [PubMed: 15169928]
3. Gartlon J, Szekeres P, Pullen M, Sarau HM, Aiyar N, Shabon U, et al. Localisation of NMU1R and NMU2R in human and rat central nervous system and effects of neuromedin-U following central administration in rats. Psychopharmacology (Berl). 2004; 177:1–14. [PubMed: 15205870]
4. Guan XM, Yu H, Jiang Q, Van Der Ploeg LH, Liu Q. Distribution of neuromedin U receptor subtype 2 mRNA in the rat brain. Brain Res Gene Expr Patterns. 2001; 1:1–4. [PubMed: 15018811]
5. Howard AD, Wang R, Pong SS, Mellin TN, Strack A, Guan XM, et al. Identification of receptors for neuromedin U and its role in feeding. Nature. 2000; 406:70–74. [PubMed: 10894543]
6. Hosoya M, Moriya T, Kawamata Y, Ohkubo S, Fujii R, Matsui H, et al. Identification and functional characterization of a novel subtype of neuromedin U receptor. J Biol Chem. 2000; 275:29528–29532. [PubMed: 10887190]
7. Budhiraja S, Chugh A. Neuromedin U: physiology, pharmacology and therapeutic potential. Fundam Clin Pharmacol. 2009; 23:149–157. [PubMed: 19645813]
8. Volkow ND, Wang GJ, Tomasi D, Baler RD. The addictive dimensionality of obesity. Biol Psychiatry. 2013; 73:811–818. [PubMed: 23374642]
9. Volkow ND, Wang GJ, Tomasi D, Baler RD. Obesity and addiction: neurobiological overlaps. Obes Rev. 2013; 14:2–18. [PubMed: 23016694]
10. Stice E, Figlewicz DP, Gosnell BA, Levine AS, Pratt WE. The contribution of brain reward circuits to the obesity epidemic. Neurosci Biobehav Rev. 2013; 37:2047–2058. [PubMed: 23237885]
11. Domin J, Ghatei MA, Chohan P, Bloom SR. Characterization of neuromedin U like immunoreactivity in rat, porcine, guinea-pig and human tissue extracts using a specific radioimmunoassay. Biochem Biophys Res Commun. 1986; 140:1127–1134. [PubMed: 3778484]
12. Thomas MJ, Kalivas PW, Shaham Y. Neuroplasticity in the mesolimbic dopamine system and cocaine addiction. Br J Pharmacol. 2008; 154:327–342. [PubMed: 18345022]
13. Steketee JD, Kalivas PW. Drug wanting: behavioral sensitization and relapse to drug-seeking behavior. Pharmacol Rev. 2011; 63:348–365. [PubMed: 21490129]
14. Koob GF, Volkow ND. Neurocircuitry of addiction. Neuropsychopharmacology. 2010; 35:217–238. [PubMed: 19710631]

15. Guillem K, Ahmed SH, Peoples LL. Escalation of cocaine intake and incubation of cocaine seeking are correlated with dissociable neuronal processes in different accumbens subregions. Biol Psychiatry. 2014; 76:31–39. [PubMed: 24120118]
16. Loweth JA, Tseng KY, Wolf ME. Adaptations in AMPA receptor transmission in the nucleus accumbens contributing to incubation of cocaine craving. Neuropharmacology. 2014; 76(Pt B): 287–300. [PubMed: 23727437]
17. Cadet JL, Brannock C, Krasnova IN, Ladenheim B, McCoy MT, Chou J, et al. Methamphetamine-induced dopamine-independent alterations in striatal gene expression in the 6-hydroxydopamine hemiparkinsonian rats. PLoS One. 2010; 5:e15643. [PubMed: 21179447]
18. Johnson C, Drgon T, Liu QR, Walther D, Edenberg H, Rice J, et al. Pooled association genome scanning for alcohol dependence using 104,268 SNPs: validation and use to identify alcoholism vulnerability loci in unrelated individuals from the collaborative study on the genetics of alcoholism. Am J Med Genet B Neuropsychiatr Genet. 2006; 141B:844–853. [PubMed: 16894614]
19. Noori HR, Spanagel R, Hansson AC. Neurocircuitry for modeling drug effects. Addict Biol. 2012; 17:827–864. [PubMed: 22978651]
20. Ferguson SM, Eskenazi D, Ishikawa M, Wanat MJ, Phillips PE, Dong Y, et al. Transient neuronal inhibition reveals opposing roles of indirect and direct pathways in sensitization. Nat Neurosci. 2011; 14:22–24. [PubMed: 21131952]
21. Baude A, Nusser Z, Molnár E, McIlhinney RA, Somogyi P. High-resolution immunogold localization of AMPA type glutamate receptor subunits at synaptic and non-synaptic sites in rat hippocampus. Neuroscience. 1995; 69:1031–1055. [PubMed: 8848093]
22. Chen L, Boyes J, Yung WH, Bolam JP. Subcellular localization of GABAB receptor subunits in rat globus pallidus. J Comp Neurol. 2004; 474:340–352. [PubMed: 15174078]
23. Medin T, Owe SG, Rinholm JE, Larsson M, Sagvolden T, Storm-Mathisen J, et al. Dopamine D5 receptors are localized at asymmetric synapses in the rat hippocampus. Neuroscience. 2011; 192:164–171. [PubMed: 21749912]
24. Carlton SM, Hayes ES. Dynorphin A(1–8) immunoreactive cell bodies, dendrites and terminals are postsynaptic to calcitonin gene-related peptide primary afferent terminals in the monkey dorsal horn. Brain Res. 1989; 504:124–128. [PubMed: 2574618]
25. Hayes ES, Carlton SM. Primary afferent interactions: analysis of calcitonin gene-related peptide-immunoreactive terminals in contact with unlabeled and GABA-immunoreactive profiles in the monkey dorsal horn. Neuroscience. 1992; 47:873–896. [PubMed: 1579216]
26. Benzon CR, Johnson SB, McCue DL, Li D, Green TA, Hommel JD. Neuromedin U receptor 2 knockdown in the paraventricular nucleus modifies behavioral responses to obesogenic high-fat food and leads to increased body weight. Neuroscience. 2014; 258:270–279. [PubMed: 24269937]
27. Bolte S, Cordelières FP. A guided tour into subcellular colocalization analysis in light microscopy. J Microsc. 2006; 224:213–232. [PubMed: 17210054]
28. Tsai W-H. Moment-preserving thresholding: a new approach. Computer Vision Graphics and Image Processing. 1985; 29:377–393.
29. Kasper JM, Booth RG, Peris J. Serotonin-2C receptor agonists decrease potassium-stimulated GABA release in the nucleus accumbens. Synapse. 2015; 69:78–85. [PubMed: 25382408]
30. Huang M, Panos JJ, Kwon S, Oyamada Y, Rajagopal L, Meltzer HY. Comparative effect of lurasidone and blonanserin on cortical glutamate, dopamine, and acetylcholine efflux: role of relative serotonin (5-HT)2A and DA D2 antagonism and 5-HT1A partial agonism. J Neurochem. 2014; 128:938–949. [PubMed: 24164459]
31. Filip M, Bubar MJ, Cunningham KA. Contribution of serotonin (5-hydroxytryptamine; 5-HT) 5-HT2 receptor subtypes to the hyperlocomotor effects of cocaine: acute and chronic pharmacological analyses. J Pharmacol Exp Ther. 2004; 310:1246–1254. [PubMed: 15131246]
32. Land BB, Narayanan NS, Liu RJ, Gianessi CA, Brayton CE, Grimaldi DM, et al. Medial prefrontal D1 dopamine neurons control food intake. Nat Neurosci. 2014; 17:248–253. [PubMed: 24441680]
33. Paxinos, G.; Watson, C. The Rat Brain in Stereotaxic Coordinates. Sixth. Academic Press; 2007.
34. Ziv NE, Garner CC. Cellular and molecular mechanisms of presynaptic assembly. Nat Rev Neurosci. 2004; 5:385–399. [PubMed: 15100721]

35. Larsson M, Broman J. Pathway-specific bidirectional regulation of Ca2+/calmodulin-dependent protein kinase II at spinal nociceptive synapses after acute noxious stimulation. J Neurosci. 2006; 26:4198–4205. [PubMed: 16624940]
36. Harris KM, Weinberg RJ. Ultrastructure of synapses in the mammalian brain. Cold Spring Harb Perspect Biol. 2012; 4
37. Baumert M, Maycox PR, Navone F, De Camilli P, Jahn R. Synaptobrevin: an integral membrane protein of 18,000 daltons present in small synaptic vesicles of rat brain. EMBO J. 1989; 8:379–384. [PubMed: 2498078]
38. Di Chiara G, Bassareo V, Fenu S, De Luca MA, Spina L, Cadoni C, et al. Dopamine and drug addiction: the nucleus accumbens shell connection. Neuropharmacology. 2004; 47(Suppl 1):227–241. [PubMed: 15464140]
39. Xi ZX, Ramamoorthy S, Shen H, Lake R, Samuvel DJ, Kalivas PW. GABA transmission in the nucleus accumbens is altered after withdrawal from repeated cocaine. J Neurosci. 2003; 23:3498–3505. [PubMed: 12716959]
40. Grotewold SK, Wall VL, Goodell DJ, Hayter C, Bland ST. Effects of cocaine combined with a social cue on conditioned place preference and nucleus accumbens monoamines after isolation rearing in rats. Psychopharmacology (Berl). 2014; 231:3041–3053. [PubMed: 24553577]
41. Andrews CM, Lucki I. Effects of cocaine on extracellular dopamine and serotonin levels in the nucleus accumbens. Psychopharmacology (Berl). 2001; 155:221–229. [PubMed: 11432683]
42. Torregrossa MM, Kalivas PW. Microdialysis and the neurochemistry of addiction. Pharmacol Biochem Behav. 2008; 90:261–272. [PubMed: 17928041]
43. Neisewander JL, Cheung TH, Pentkowski NS. Dopamine D3 and 5-HT1B receptor dysregulation as a result of psychostimulant intake and forced abstinence: Implications for medications development. Neuropharmacology. 2014; 76(Pt B):301–319. [PubMed: 23973315]
44. Wren AM, Small CJ, Abbott CR, Jethwa PH, Kennedy AR, Murphy KG, et al. Hypothalamic actions of neuromedin U. Endocrinology. 2002; 143:4227–4234. [PubMed: 12399416]
45. Nakazato M, Hanada R, Murakami N, Date Y, Mondal MS, Kojima M, et al. Central effects of neuromedin U in the regulation of energy homeostasis. Biochem Biophys Res Commun. 2000; 277:191–194. [PubMed: 11027662]
46. Ikeda H, Adachi K, Fujita S, Tomiyama K, Saigusa T, Kobayashi M, et al. Investigating complex basal ganglia circuitry in the regulation of motor behaviour, with particular focus on orofacial movement. Behav Pharmacol. 2015; 26:18–32. [PubMed: 25485640]
47. Salegio EA, Samaranch L, Kells AP, Mittermeyer G, San Sebastian W, Zhou S, et al. Axonal transport of adeno-associated viral vectors is serotype-dependent. Gene Ther. 2013; 20:348–352. [PubMed: 22418061]
48. San Sebastian W, Samaranch L, Heller G, Kells AP, Bringas J, Pivirotto P, et al. Adeno-associated virus type 6 is retrogradely transported in the non-human primate brain. Gene Ther. 2013; 20:1178–1183. [PubMed: 24067867]
49. Wydra K, Golembiowska K, Zaniewska M, Kamińska K, Ferraro L, Fuxe K, et al. Accumbal and pallidal dopamine, glutamate and GABA overflow during cocaine self-administration and its extinction in rats. Addict Biol. 2013; 18:307–324. [PubMed: 23311632]
50. Sorg BA, Guminski BJ, Hooks MS, Kalivas PW. Cocaine alters glutamic acid decarboxylase differentially in the nucleus accumbens core and shell. Brain Res Mol Brain Res. 1995; 29:381–386. [PubMed: 7609627]
51. Kennedy PJ, Feng J, Robison AJ, Maze I, Badimon A, Mouzon E, et al. Class I HDAC inhibition blocks cocaine-induced plasticity by targeted changes in histone methylation. Nat Neurosci. 2013; 16:434–440. [PubMed: 23475113]
52. McDevitt RA, Tiran-Cappello A, Shen H, Balderas I, Britt JP, Marino RA, et al. Serotonergic versus nonserotonergic dorsal raphe projection neurons: differential participation in reward circuitry. Cell Rep. 2014; 8:1857–1869. [PubMed: 25242321]
53. Bang SJ, Commons KG. Forebrain GABAergic projections from the dorsal raphe nucleus identified by using GAD67-GFP knock-in mice. J Comp Neurol. 2012; 520:4157–4167. [PubMed: 22605640]

54. Vasudeva RK, Lin RC, Simpson KL, Waterhouse BD. Functional organization of the dorsal raphe efferent system with special consideration of nitrergic cell groups. J Chem Neuroanat. 2011; 41:281–293. [PubMed: 21640185]

55. Lobo MK, Nestler EJ. The striatal balancing act in drug addiction: distinct roles of direct and indirect pathway medium spiny neurons. Front Neuroanat. 2011; 5:41. [PubMed: 21811439]

56. Martin TA, Jayanthi S, McCoy MT, Brannock C, Ladenheim B, Garrett T, et al. Methamphetamine causes differential alterations in gene expression and patterns of histone acetylation/ hypoacetylation in the rat nucleus accumbens. PLoS One. 2012; 7:e34236. [PubMed: 22470541]

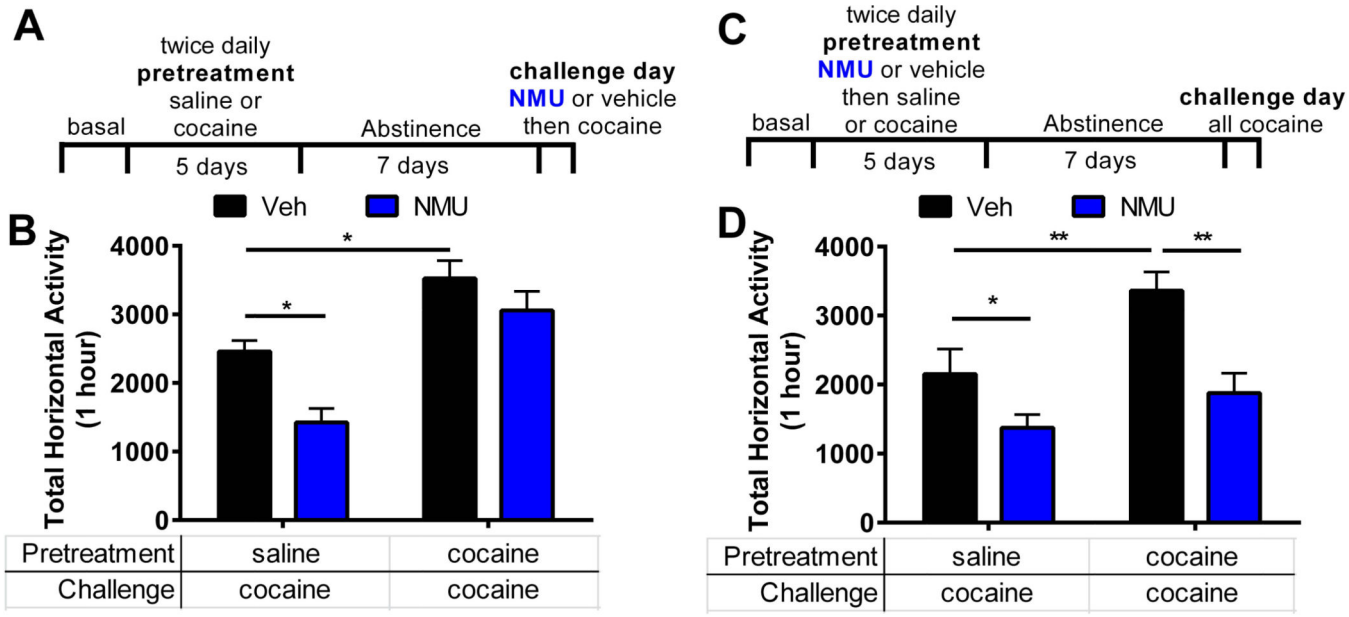

Figure 1.

NMUR2 is expressed synaptically in the NAcSh. (a) Brain slice illustration (left) showing the site in the NAcSh where confocal microscopy images (63×) of NMUR2 immunofluorescence (right) were taken. Scale bar 5 μm. (b) Representative images of electron microscopy in the NAcSh with NMUR2 immunogold staining highlighted by blue arrows. Synapses can be seen as the dark lines of electron density. Scale bar 100 nm. (c) Summary of the synaptic localization of NMUR2 from 166 electron microscopy images. Proximity of a gold piece to a synapse was defined as follows: synaptic is < 50 nm from synapse, perisynaptic is 50 to 150 nm from synapse, and nonsynaptic is > 150 nm. Presynaptic and postsynaptic localization was determined by identification of clear vesicles and the postsynaptic density, respectively.

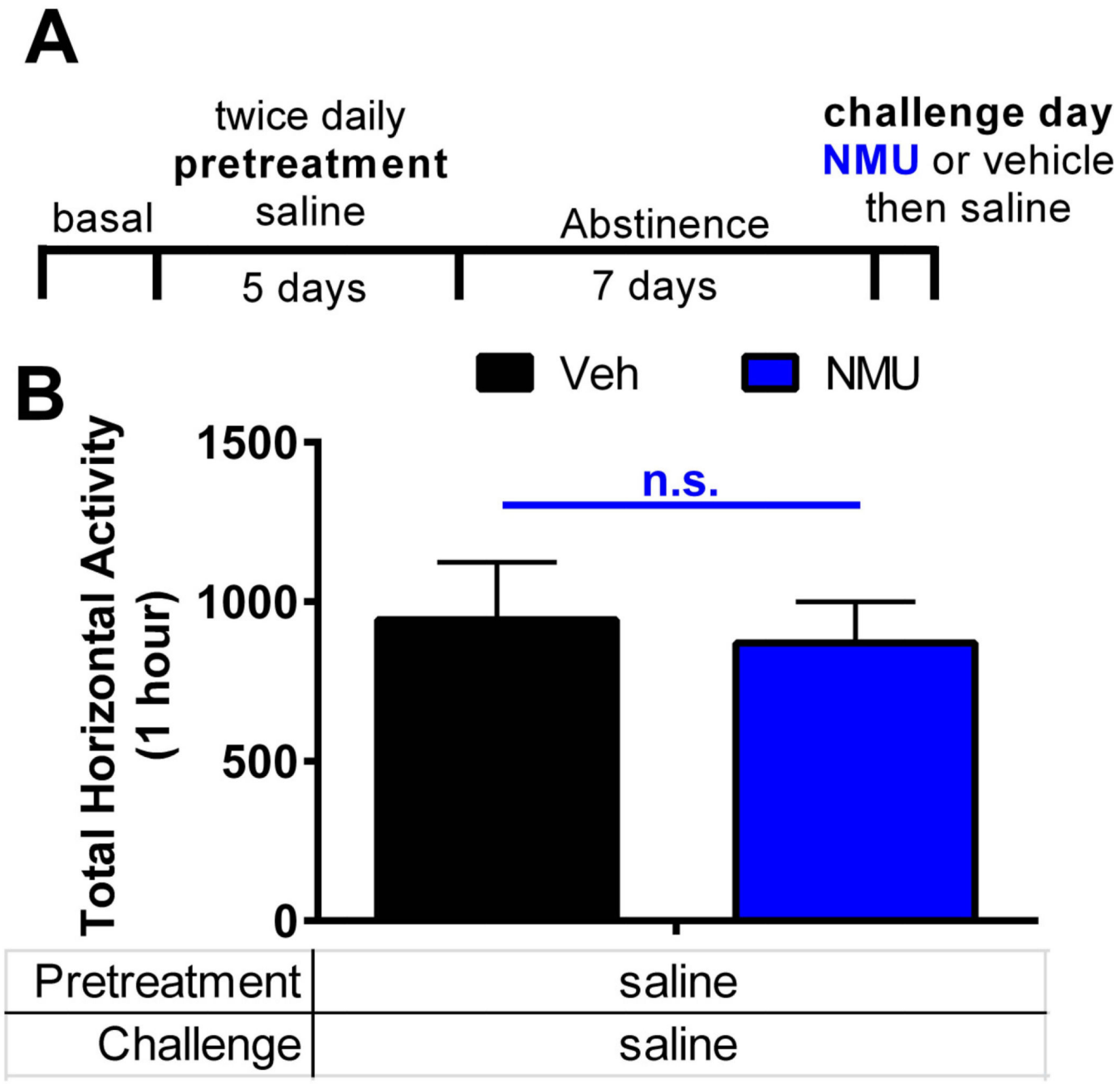

Figure 2.

Accumbal NMUR2 is primarily expressed on DRN projections compared to tVTA, AMG or CPu projections. (a) Illustration depicting the microinjection of viral vector tracer into a brain region (DRN, tVTA, AMG, or CPu) and confocal images with 63× objective in the NAcSh (green square). (b) Quantification of the colocalization of NMUR2 with the tracer from the various brain regions (n = 4 per group). Bar graph shows mean ± s.e.m. *$p < 0.05$ compared to all other groups. (c) Representative confocal images that were quantified in (b). NMUR2 is shown in cyan and tracer in green. Scale bar = 5 μm.

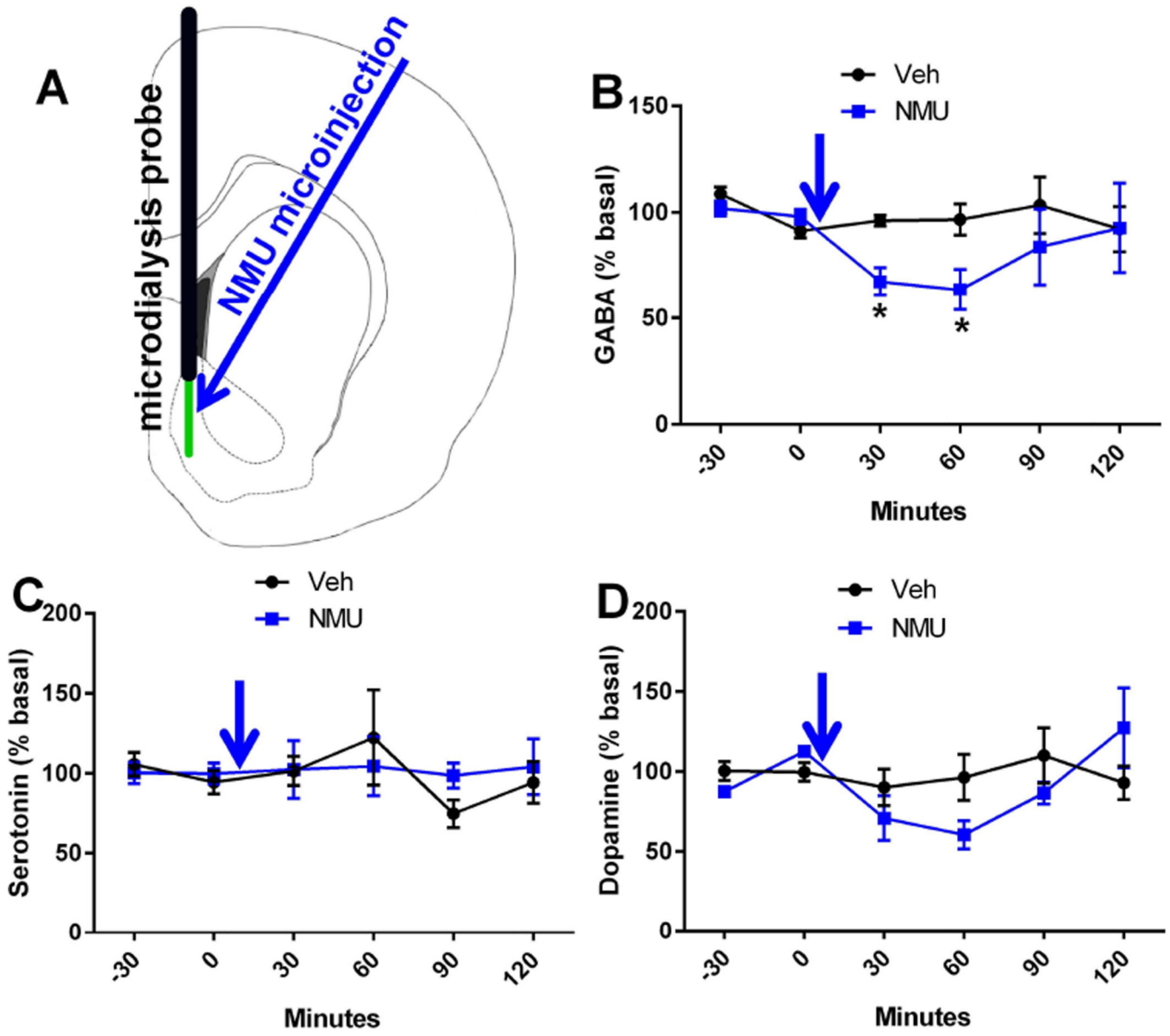

Figure 3.

Accumbal NMUR2 is expressed predominantly on GABAergic neurons. (a) Quantification of NMUR2 colocalization with the neuronal markers GAD67, TPH, and TH (n = 4 per group). Bar graph shows mean ± s.e.m. $^{**}p < 0.05$ compared to all other groups. (b) Representative confocal images that were quantified in (a). NMUR2 is shown in cyan and neuronal markers in red. Scale bar = 5 μm.

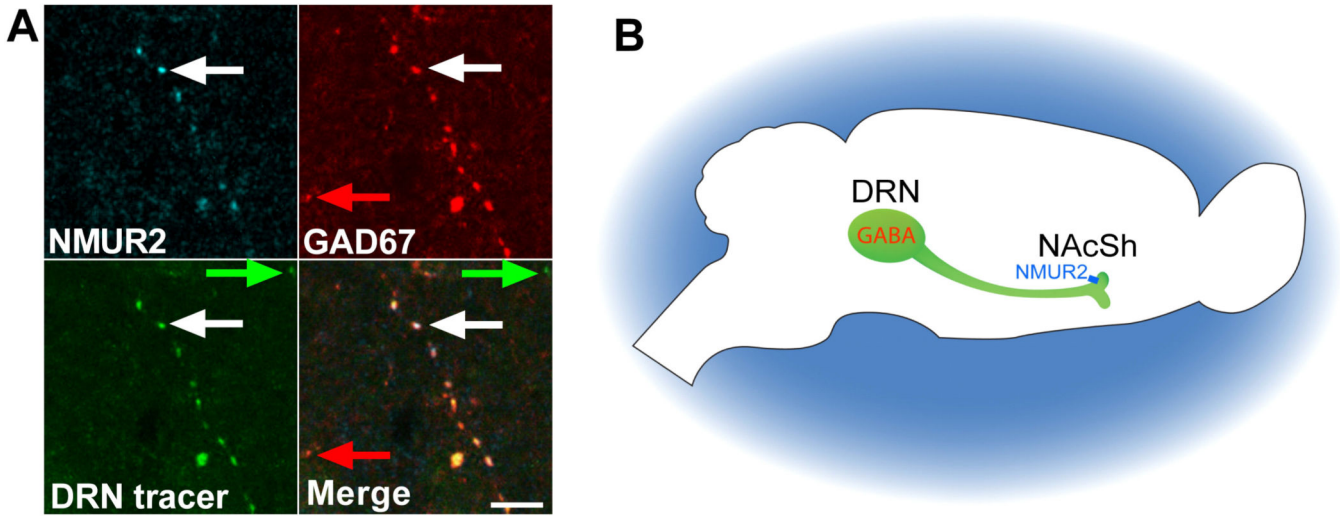

Figure 4.

NMUR2 in the NAcSh is expressed on GABAergic neurons projecting from the DRN. (a) Confocal microscopy image with 63× objective showing accumbal NMUR2 (cyan), viral tracer from the DRN (green), and GAD67 (red) colocalizing in the merge. Example of colocalization is in white arrows and examples of noncolocalization are in red and green arrows. Scale bar = 5 μm. (b) Illustration summarizing the proposed pathway.

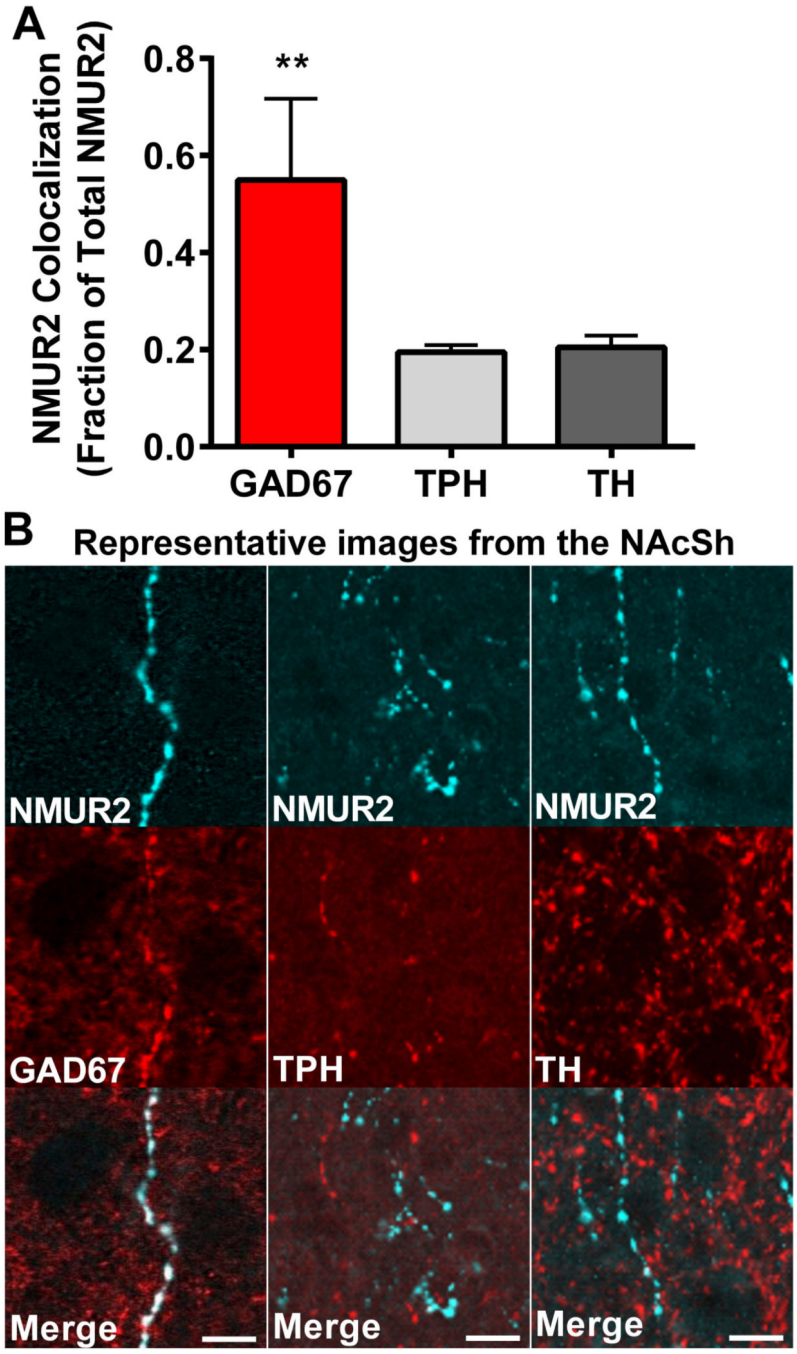

Figure 5.

NMU attenuates GABA but not serotonin or dopamine release. (a) Diagram depicting the placement of the microdialysis probe active length (green) and the microinjection site (blue arrow). (b–d) Concentrations of extracellular neurotransmitters expressed as a percentile of the basal (time points - 30 and 0) concentration over time. Blue arrow represents when the microinjection of NMU or vehicle was administered. GABA concentrations were significantly different (n = 6–7 per group) while there was no significant main effects in

either serotonin or dopamine. Line graphs show mean ± s.e.m.*$p < 0.05$ compared to control group.

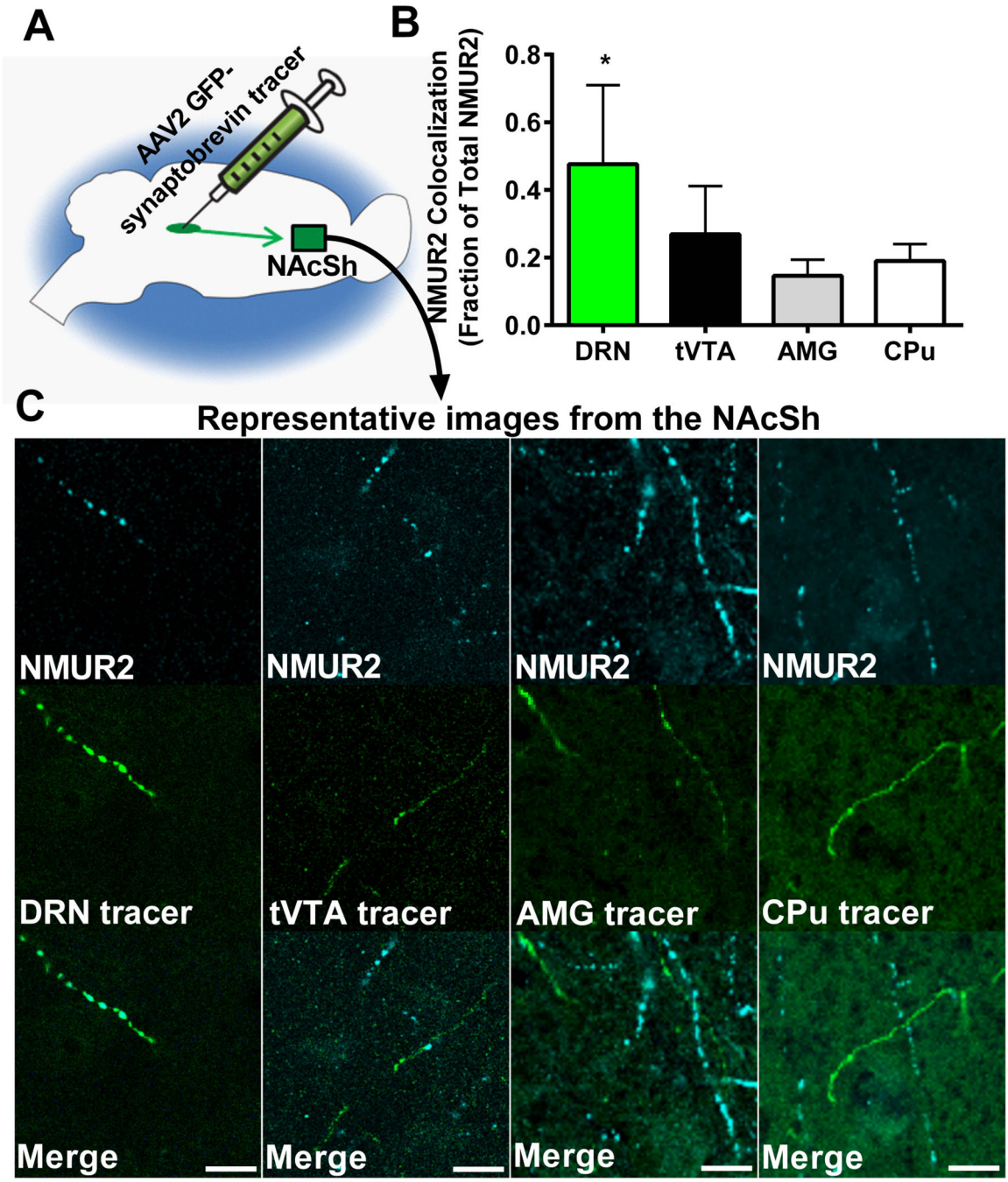

Figure 6.

NMU in the NAcSh does not alter basal locomotor activity. (a) Schematic of experimental timeline. Saline was injected (i.p.) twice per day for 5 days during pretreatment. Rats received no treatments for 7 days. On challenge day, rats received a bilateral microinjection of NMU (0.3 nmol per side) or vehicle directly into the NAcSh. Following the microinjection, rats received saline and locomotor activity was measured. (b) Challenge day locomotor activity measured by total horizontal beam breaks immediately following saline injection (n = 7–8 per group). Bar graphs show mean ± s.e.m. * $p < 0.05$ by *t*-test.

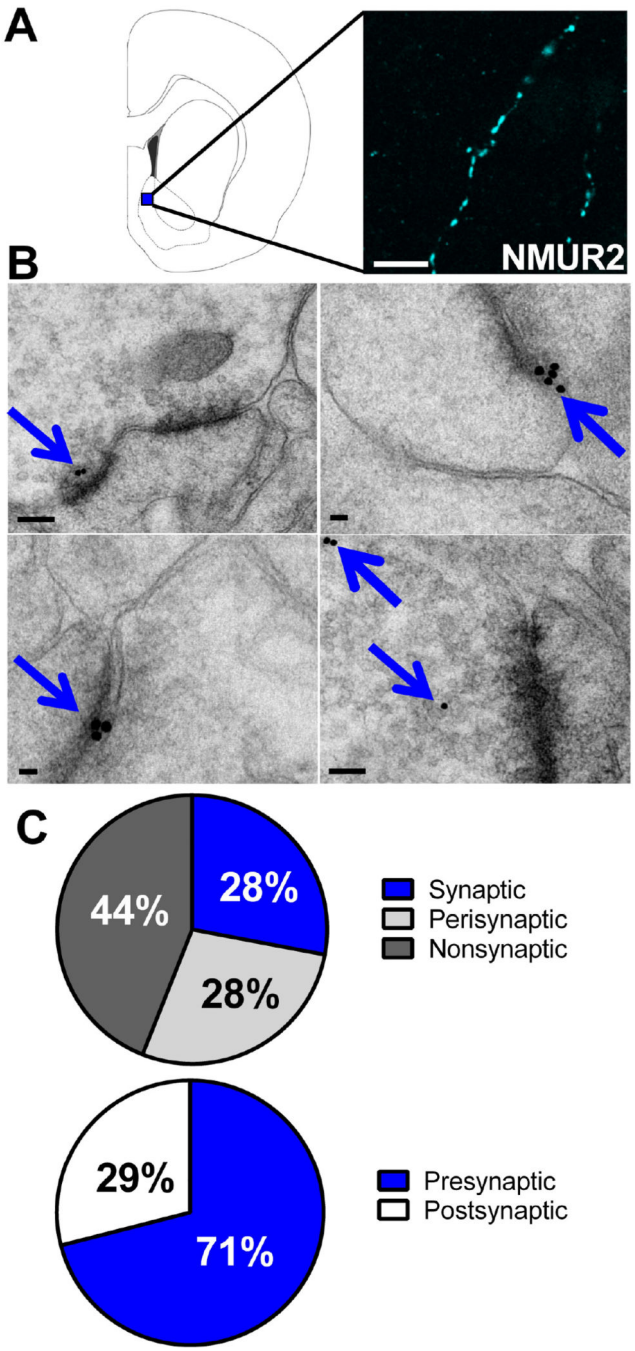

Figure 7.

NMU administered during initiation but not expression blocks sensitization. (a) Schematic of experimental timeline for the expression of cocaine sensitization. Cocaine or saline was injected (i.p.) twice per day for 5 days during pretreatment. Rats received no treatments for 7 days. On challenge day, rats received a bilateral microinjection of NMU (0.3 nmol per side) or vehicle directly into the NAcSh. Following the microinjection, all rats received cocaine and locomotor activity was measured. (b) Challenge day locomotor activity measured by total horizontal beam breaks immediately following cocaine injection (n = 7–8 per group).

(c) Schematic of experimental timeline for initiation of cocaine sensitization. NMU or vehicle is administered throughout pretreatment and not on challenge day. (d) Challenge day locomotor activity (n = 7–10 per group). Bar graphs show mean ± s.e.m. * $p < 0.05$ and ** $p < 0.01$ between groups.

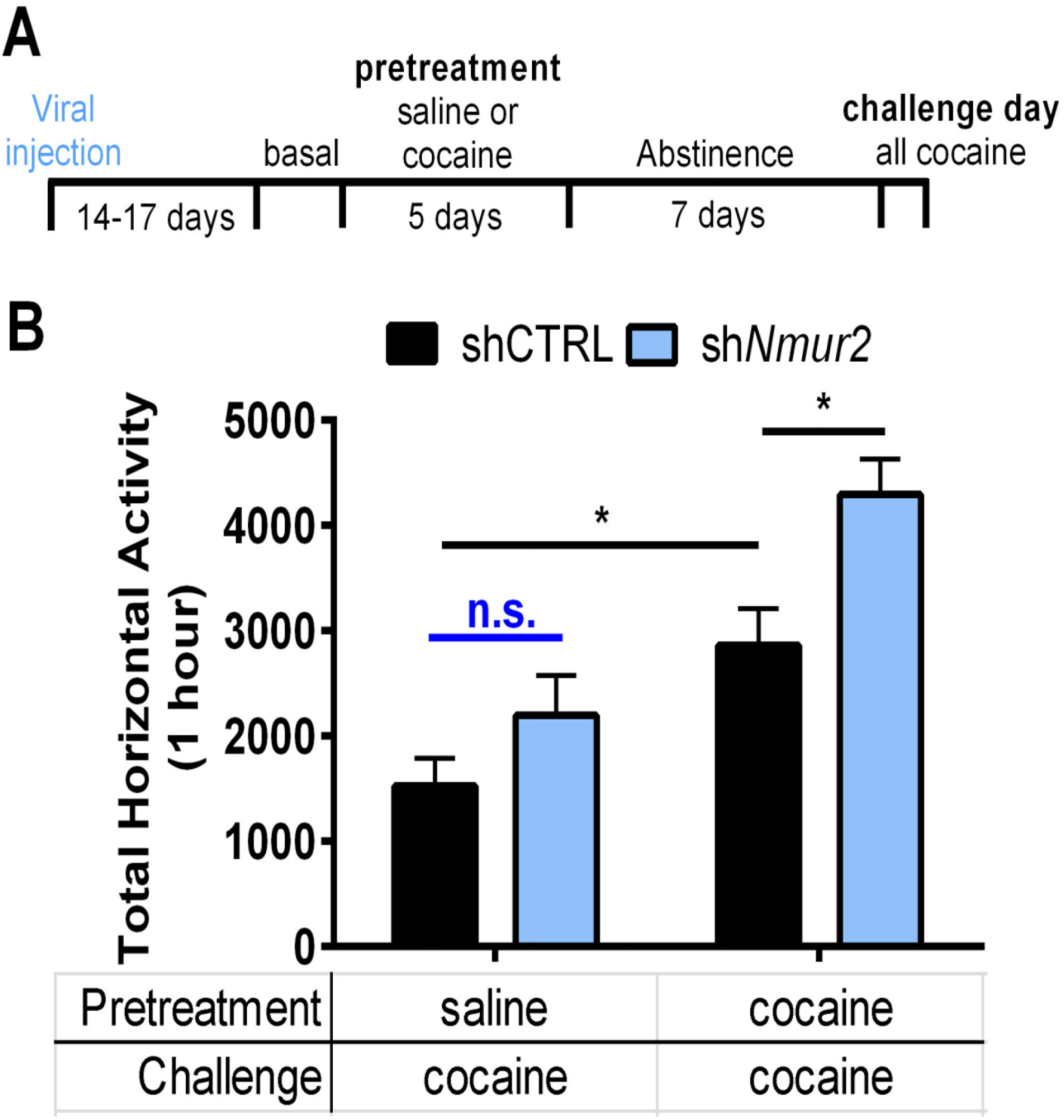

Figure 8.

Knockdown of presynaptic NMUR2 in the NAcSh augments cocaine sensitization. (a) Schematic of experimental timeline for cocaine sensitization after virus was allowed to reach maximal expression. (b) Challenge day locomotor activity measured by total horizontal beam breaks immediately following cocaine injection (n = 8–10 per group). Bar graph shows mean ± s.e.m. *$p < 0.05$ between groups.